Hierarchical Tapered Bar Elements

Undergoing Axial Deformation

N. Ganesan and S. K. Thampi

GE Government Services, Houston, Texas

ABSTRACT: A method is described to model the dynamics of tapered axial bars of various cross sections based on the well-known Craig/Bampton component mode synthesis technique. This element is formed in terms of the static constraint modes and interface restrained normal modes. This is in contrast with the finite elements as implemented in NASTRAN where the interface restrained normal modes are neglected. These normal modes are in terms of Bessel functions. Restoration of a few of these modes leads to higher accuracy with fewer generalized coordinates. The proposed models are hierarchical so that all lower order element matrices are embedded in higher order element matrices. The advantages of this formulation compared to standard NASTRAN truss element formulation are demonstrated through simple numerical examples.

1. Introduction: Tapered bars and beams have high strength to weight ratios as well as architectural advantages. They are frequently employed to model structures in diverse applications, such as ship masts, turbine blades, chimney structures or complex frame constructions. NASA (Langley) has tested a truss structure which is made from tapered members to be used in space applications [1]. The technical literature on tapered beams is indeed vast with a long history [2-10]. Tapered beam finite elements are either simple elements (e.g., Lindberg[2], Rouch/Kao[3]) having two degrees of freedom at each end or higher order elements (e.g., Thomas/Dokumaci[4], To[5]) having more than four degrees of freedom. Ovunck[6], Avakian/Beskos[7], Gupta[8], Banerjee/Williams[9] and Spyrakos/Chen[10] have used frequency dependent finite elments in their analysis of tapered bars. Banerjee/Williams[9] have developed exact dynamic stiffness matrices for Bernoulli-Euler beams. However the approach in References [6-10] involves the unknown frequencies of the overall structure. The general framework developed by Engels[11] and applied in References [12-14] allows for the derivation of hierarchical finite elements for any type of structural element. This approach does not require the prior knowledge of system frequencies, thus overcoming the need for an iterative procedure to compute the structural response. In the present paper, a dynamic finite element model for a certain class of tapered bars with loads acting only in the axial direction is developed. The element matrices are presented in parametric form and can be easily extended to formulate the finite elments for a wide variety of tapered bars covering most practical cases. The convergence properties of this dynamic finite element, when compared to the regular finite element, are examined using numerical examples.

2. Assumed Modes Method: The Lagrangian elastic displacement vector $e(x, y, z, t)$ for a generic element can be written as the sum of two separate displacement vectors e_I

and $\bar{e}$.

$$e = e_I + \bar{e} \qquad (1)$$

where e_I is a quasi-static displacement vector due to the interface displacements q_I and is expressed as a linear combination of static constraint modes ϕ_I,

$$e_I = \phi_I \, q_I \qquad (2)$$

The second part $\bar{e}$ represents the remainder of the total displacement vector e. It is that part of e which is measured relative to e_I by an absolute observer. Clearly, $\bar{e}$ vanishes at the q_I coordinates and therefore can be expressed as a linear combination of assumed modes $\bar{\phi}$ which are restrained at those q_I coordinates

$$\bar{e} = \bar{\phi} \, \bar{q} \qquad (3)$$

The vector $\bar{q}$ represents a set of generalized coordinates to be determined as part of the solution. One example of $\bar{\phi}$ modes are the normal modes of the element E restrained at the q_I coordinates. It should be stressed that although restrained normal modes have often unique advantages, they are only one of many possible sets. In fact, $\bar{\phi}$ modes need only be restricted to admissible functions that vanish at the q_I coordinates. Substituting Eqs. (2) and (3) into Eq. (1) yields

$$e = [\phi_I \; \bar{\phi}] \left\{ \begin{array}{c} q_I \\ \bar{q} \end{array} \right\} \stackrel{\text{def}}{=} \phi \, q \qquad (4)$$

so that e is written in terms of a linear combination of two sets of assumed modes: (1) static constraint modes and (2) interface restrained assumed modes. It should be noted that the representation of e in Eq. (4) is complete in the sense that any degree of accuracy is theoretically possible as long as enough $\bar{\phi}$ modes are added.

In the standard consistent mass matrix approach, the elastic displacement vector e over the element is represented as a linear combination of interpolation or shape functions. In fact, these shape functions are identical to the static constraint modes ϕ_I and therefore e is approximated by e_I as in Eq. (1). The standard finite element approach therefore totally neglects the displacement $\bar{e}$ in Eq. (1). Ignoring $\bar{e}$ leads directly to a deterioration of the modal content of a typical finite element model. One way to ensure better convergence to a desired model fidelity is suggested by Eq. (4) and leads to dynamic finite element models. Instead of totally neglecting the $\bar{e}$ displacement, one could retain a limited number of $\bar{q}$ coordinates, thereby improving the mass and force distribution models. Of course, adding $\bar{q}$ coordinates also increases the order of the overall model. However, this approach has three important advantages: (1) The model converges much faster, i.e., far fewer degrees of freedom are necessary to attain comparable accuracy; (2) in principle, no further subdivision of basic elements is necessary, thereby simplifying the finite element grid and (3) the model is hierarchical and therefore has all the advantages associated with this property. In addition, these finite element models are directly based on the assumed modes method which provides a sound theoretical basis.

In Reference [11] it is shown that for a linear elastic material, the element kinetic and potential energies T and V can be written as

$$T = \frac{1}{2}\dot{q}^T M \dot{q}, \quad M = \int\limits_E \phi^T \phi \; dm \tag{5}$$

$$V = \frac{1}{2}q^T K q, \quad K = \int\limits_E (B\phi)^T C (B\phi) \; dV \tag{6}$$

in which the matrix C is the material stiffness matrix and B contains the appropriate partial derivatives in x, y and z. Futhermore, the matrices M and K represent the mass and stiffness matrices of a generic finite element E. In partitioned form,

$$M = \begin{bmatrix} M_{II} & M_{IN} \\ M_{IN}^T & M_{NN} \end{bmatrix}, \quad K = \begin{bmatrix} K_{II} & 0 \\ 0 & K_{NN} \end{bmatrix} \tag{7}$$

where

$$M_{II} = \int\limits_E \phi_I^T \phi_I \; dm, \quad M_{IN} = \int\limits_E \phi_I^T \overline{\phi} \; dm, \quad M_{NN} = \int\limits_E \overline{\phi}^T \overline{\phi} \; dm \tag{8}$$

and

$$K_{II} = \int\limits_E (B\phi_I)^T C(B\phi_I) dV, \quad K_{NN} = \int\limits_E (B\overline{\phi})^T C(B\overline{\phi}) dV \tag{9}$$

Note that the K_{IN} partition is always zero, which means that no stiffness coupling exists between q_I and $\overline{q}$.

At this point, a few remarks are in order. First, the matrices M_{II} and K_{II} represent the standard finite element consistent mass and stiffness matrices for the element E. The consistent mass matrix approach represents in fact a static condensation or Guyan reduction whereby all noninterface degrees of freedom are eliminated. Secondly, if the interface restrained normal modes are used for the columns of $\overline{\phi}$, then the present approach is identical to the Craig/Bampton component mode synthesis procedure as applied to a finite element. It should be emphasized that the element E is generic. This means that the proposed approach is valid, at least in theory, for any type of element. In the present paper, this general procedure will be applied to the special case of the tapered bars.

3. Tapered Bars: The hierarchical stiffness and mass matrices of the tapered bar are obtained by solving the governing equations of motion for displacement. Figure (1) represents linear tapered bar ab with a straight centroidal axis and the directions of the principal axes being the same for all crossections. The cross sectional area $A(x)$ is given by

$$A(x) = A_a \left(1 + c\frac{x}{L}\right)^n \tag{10}$$

where $c = d_b/d_a - 1$ and A_i, d_i $(i = a, b)$ denote the cross sectional area and the depth respectively. $c > -1$ otherwise the beam tapers to zero between its ends and L is the length of the bar.

Although the formulation is valid for any $n > 0$, many practical cases of tapered bars arise when n is one or two, see Figure (2). If the geometrical properties of the element at both ends are given, the shape function for n can be derived as

$$n = \frac{log(A_b/A_a)}{log(d_b/d_a)} \quad (11)$$

For bars of closed box or I-section of constant width and varying depth, n is not an integer and will vary slightly from E-q. (10) at all x other than the two ends. But the deviations are usually within one percent of the exact values.
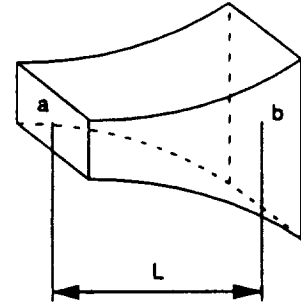

Figure 1.

Tapered Element

4. Static Constraint Modes: Consider the axial bar element as illustrated in Figure (1). The bar is assumed to undergo vibration along its own axis and as a rigid body can only move along that same axis. The interface displacements are defined as $q_1(t) = u(0, t)$ and $q_2(t) = u(L, t)$, i.e., $\mathbf{q}_I = [\ q_1\ \ q_2\ ]^T$ and the displacement vector e is considered to have only one component, i.e., u. Eq. (4) is therefore written as

$$u = \lfloor\ \phi_1\ \ \phi_2\ \rfloor \mathbf{q}_I + \overline{\phi}\ \overline{\mathbf{q}} \quad (12)$$
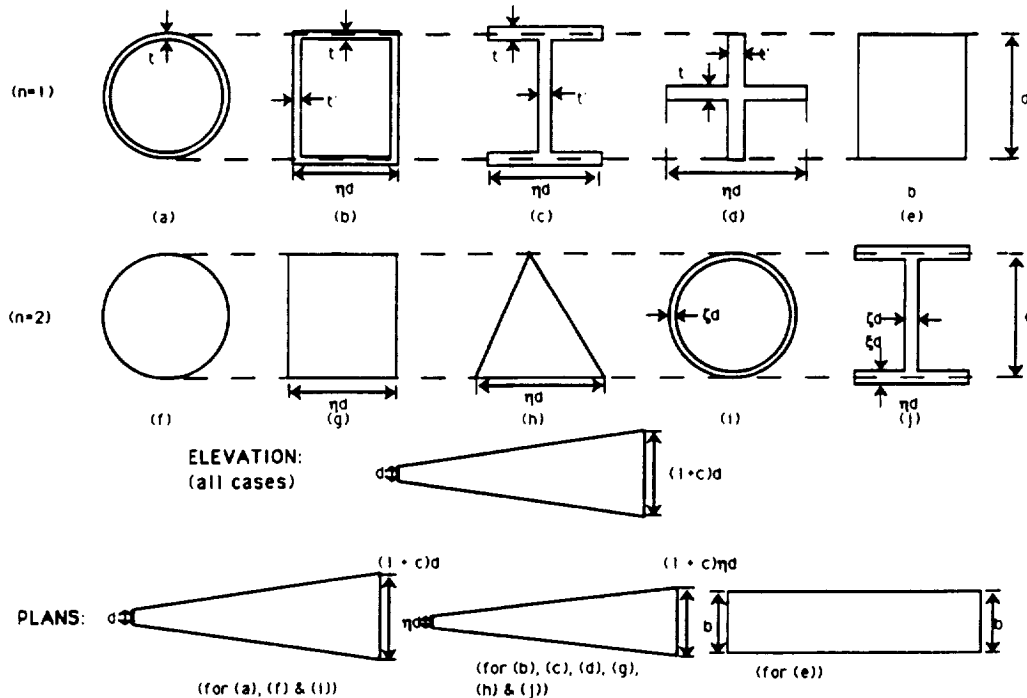

Figure 2. Sample Cross Sections

The static constraint modes, ϕ_i can be computed from the differential equation for the axial deformation u at x from end a of the tapered bar,

$$\frac{d}{dx}\left\{EA(x)\frac{du}{dx}\right\} = 0 \tag{13}$$

where E is Young's modulus. Integration of Eq. (13) gives,

$$EA(x)\frac{du}{dx} = C_1 \tag{14}$$

Substituting for $A(x)$ from Eq. (10) and setting $\xi = 1 + c\frac{x}{L}$ gives

$$\frac{du}{d\xi} = \frac{C_1 L}{EA_a c}\frac{1}{\xi^n} \tag{15}$$

Integrating Eq. (15) again,

$$u = \frac{C_1 L}{EA_a c}f(\xi) + C_2 \tag{16}$$

where

$$f(\xi) = -\frac{1}{(n-1)\xi^{n-1}} \text{ for } n \neq 1 \tag{17}$$
$$= \ln \xi \text{ for } n = 1$$

The appropriate boundary conditions for the computation of static constraint modes are given by

$$q_1 = 1, \ q_2 = 0 \tag{18}$$
$$q_1 = 0, \ q_2 = 1$$

The resulting static constraint modes are

$$\phi_1 = \frac{f(\xi) - f(1+c)}{f(1) - f(1+c)}, \quad \phi_2 = \frac{f(1) - f(\xi)}{f(1) - f(1+c)} \tag{19}$$

Note that these constraint modes are in fact the shape functions used in the stiffness matrix of the tapered bar.

At this point, enough information exists to compute M_{II} and K_{II} from Eqs. (8–9). Indeed, for the tapered bar, the kinetic and potential energies T and V are given as

$$T = \frac{1}{2}\int_0^L \rho A(x)\left(\frac{\partial u}{\partial t}\right)^2 dx, \ V = \frac{1}{2}\int_0^L EA(x)\left(\frac{\partial u}{\partial x}\right)^2 dx \tag{20}$$

Substituting Eq. (12) into Eq. (20) gives

$$M_{II} = \int_0^L \rho A(x)\phi_I^T \phi_I dx, \ K_{II} = \int_0^L EA(x)\frac{d\phi_I}{dx}^T \frac{d\phi_I}{dx}dx \tag{21}$$

128

When $n = 1$, the explicit expressions for K_{II} and M_{II} are defined as

$$K_{II} = \frac{EA_a}{L} \frac{c}{\ln(1+c)} \begin{bmatrix} 1 & -1 \\ -1 & 1 \end{bmatrix}, \quad M_{II} = \begin{bmatrix} m_{11} & m_{12} \\ m_{21} & m_{22} \end{bmatrix} \qquad (22)$$

where

$$m_{11} = \frac{\rho A_a L}{4c\ln^2(1+c)} \left[-2\ln^2(1+c) - 2\ln(1+c) + c^2 + 2c \right]$$

$$m_{12} = m_{21} = \frac{\rho A_a L}{4c\ln^2(1+c)} \left[(c^2 + 2c + 2)\ln(1+c) - c^2 - 2c \right] \qquad (23)$$

$$m_{22} = \frac{\rho A_a L}{4c\ln^2(1+c)} \left[2(1+c)^2(\ln^2(1+c) - \ln(1+c)) + c^2 + 2c \right]$$

The counterpart expression for K_{II} when $n \neq 1$ is given as

$$K_{II} = \frac{EA_a c(n-1)(1+c)^{n-1}}{(1+c)^{n-1} - 1} \begin{bmatrix} 1 & -1 \\ -1 & 1 \end{bmatrix} \quad (n \neq 1) \qquad (24)$$

The stifness matrix partitions K_{II} and M_{II} for $n = 2$ are evaluated as

$$K_{II} = \frac{EA_a(1+c)}{L} \begin{bmatrix} 1 & -1 \\ -1 & 1 \end{bmatrix}, \quad M_{II} = \frac{\rho A_a L}{6} \begin{bmatrix} 2 & 1+c \\ 1+c & 2(1+c)^2 \end{bmatrix} \qquad (25)$$

Because of the similarity of the governing equations between axial bars and torsional shafts, Eq. (25) can be used as the stiffness and consistent mass matrices for tapered shafts by replacing the variables A_a, E with J_a, G respectively, where J_a is the polar second moment of area and G is the shear modulus of elasticity. If it is decided that no extra $\bar{q}$ coordinates are to be retained in Eq. (4), then the procedure can be terminated at this stage.

5. Interface Restrained Normal Modes: An entire class of hierarchical models can now be created solely on the basis of choosing the interface restrained assumed modes. In this paper, the set of interface restrained normal modes is used. The normal modes and their corresponding frequencies are obtained from solving the eigenvalue problem associated with the partial differential equation,

$$\frac{\partial}{\partial x} \left\{ EA(x) \frac{\partial u}{\partial x} \right\} = \rho A(x) \frac{\partial^2 u}{\partial t^2} \qquad (26)$$

subjected to the clamped–clamped boundary conditions.

Substituting for A(x) from Eq. (10) and letting $\xi = 1 + cx/L$ gives,

$$\frac{\partial^2 u}{\partial \xi^2} + \frac{n}{\xi} \frac{\partial u}{\partial \xi} = \frac{\rho L^2}{Ec^2} \frac{\partial^2 u}{\partial t^2} \qquad (27)$$

For harmonic vibration,

$$u(\xi, t) = U(\xi) \sin \omega t \qquad (28)$$

where t denotes time and ω is the circular natural frequency. Eq. (27) is modified using Eq. (28) as

$$\frac{d^2 U}{d\xi^2} + \frac{n}{\xi} \frac{dU}{d\xi} + \omega^2 \frac{\rho L^2}{E c^2} U = 0 \qquad (29)$$

The solution of Eq. (29) when $c > 0$ is

$$U(\xi) = \xi^{\frac{1-n}{2}} \left\{ A J_{\frac{1-n}{2}}(\alpha\xi) + B Y_{\frac{1-n}{2}}(\alpha\xi) \right\} \qquad (30)$$

where J and Y are Bessel functions of the first and second kind and $\alpha = \frac{\omega L}{c} \sqrt{\frac{\rho}{E}}$.

For the case of $n = 2$, imposing the clamped–clamped boundary conditions in Eq. (30) yields the characterstic equation for the tapered bar,

$$\sin \alpha c = 0 \qquad (31)$$

The solution of Eq. (31) is

$$\omega = \frac{i\pi}{L} \sqrt{\frac{E}{\rho}}, \ i = 1, 2, \ldots, \infty \qquad (32)$$

It is noteworthy that the natural frequencies of the tapered bar with clamped ends for the case of $n = 2$ are independent of c and are in fact the same as that of uniform rods. From Eq. (30), the interface restrained normal modes for $n = 2$ becomes

$$\overline{\phi}_i = C_i \frac{\sin(\alpha\xi - \alpha)}{\xi} \qquad (33)$$

where the mass normalization constant C_i must satisfy

$$\int_1^{1+c} \rho A(\xi) \overline{\phi}_i^2(\xi) d\xi = 1 \qquad (34)$$

Substituting Eq. (33) into Eq. (34), C_i is determined as

$$C_i = \sqrt{\frac{2}{\rho A_a L}} \qquad (35)$$

From Eq. (8), the mass matrix partitions are evaluated as

$$M_{NN} = \int_0^L \rho A(x) \overline{\phi}^T \overline{\phi} dx = I, \quad M_{IN} = [m_{ji}], \quad m_{ji} = \int_0^L \rho A(x) \phi_j \overline{\phi}_i dx \qquad (36)$$

$$i = 1, 2, \ldots, \infty, \ j = 1, 2$$

130

with

$$m_{1i} = \frac{\sqrt{2\rho A_a L}}{i\pi}, \quad m_{2i} = \frac{\sqrt{2\rho A_a L}}{i\pi}(1 + c)(-1)^{i+1} \tag{37}$$

When c is set to zero, Eqs. (25) and (36) reduce to the case of uniform bars. Application of Eq. (33) into Eq. (20) gives the stiffness matrix partitions,

$$K_{IN} = 0, \quad K_{NN} = \text{Diag.}\ [\omega_1^2\ \omega_2^2 \dots] \tag{38}$$

and ω_i is given by Eq. (32). It can be seen that the tapered bar element matrices consist of very simple terms.

6. Demonstration Examples:

6.1 Tapered Cantilever: This first example is concerned with the cantilevered bar clamped at the right end, see Figure (3). The pertinent structural parameters are $E = 30 \times 10^6$ psi, $\rho g = 0.2839$ lb/in^3, $A_a = 1$ in^2, $A_b = 4$ in^2 and $L = 72$ in.

The characteristic equation of this cantilever is given by

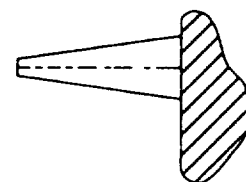$$\alpha \cos \alpha c + \sin \alpha c = 0 \tag{39}$$

Figure 3. Cantilever

Tables (1) and (2) show the number of converged frequencies to within a given percentage relative error when compared to the theoretical frequencies from Eq. (39) for different model orders n.

Note that the bar is subdivided into the requisite number of elements to arrive at the model order n in the standard finite element method as implemented in CSA–NASTRAN whereas in the hierarchical finite element model, the number of bar elements is always one and the requisite interface restrained normal modes are added to arrive at n.

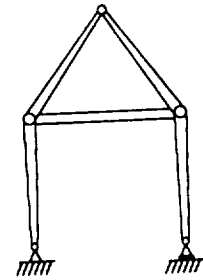**Table 1. Standard Finite Element Method**

e	n				
	8	16	24	32	40
< 1 %	1	3	4	5	6
< 5 %	3	6	8	11	14
< 10 %	4	8	12	16	20

131

Table 2. Hierarchical Finite Element Method

e	n				
	8	16	24	32	40
< 1 %	6	14	23	31	39
< 5 %	7	15	23	31	39
< 10 %	7	15	23	31	39

6.2 Planar Truss: Next, consider the planar single-bay truss as illustrated in Figure (4). The parameters are the same as in Section (6.1). The horizontal bar has a uniform cross sectional area of 4 in^2. For planar truss elements, the transverse inertia must be taken into account. This time, however, no 'exact solution' for the frequencies of the structure exists. A reference solution was obtained in two different ways: (1) by constructing a highly refined standard finite element model (2) by retaining a large number of normal modes in the hierarchical model. Both models were refined to the point where no significant change in the frequencies occured and both the models produced the same results.

Figure 4. Planar Truss

Table (3) lists the frequencies from the hierarchical finite element model when two normal modes per bar are added (i.e., $n = 16$) as compared to the reference solution. In order to achieve comparable results from standard finite element method, each bar has to be subdivided into five beam elements (i.e., $n = 66$) and consistent mass matrix has to be generated within NASTRAN.

Table 3. Frequency Comparisons For Planar Truss

Mode Number	Reference Frequency (Hz)	Computed Frequency (Hz)	Error %
2	2.606E2	2.606E2	-1.123E-2
3	2.999E2	2.999E2	-1.703E-2
5	6.958E2	6.961E2	-4.763E-2
7	1.467E3	1.468E3	-1.837E-2
9	1.757E3	1.762E3	-2.970E-1
11	2.141E3	2.172E3	-1.432
13	2.889E3	2.898E3	-3.317E-1
14	3.049E3	3.081E3	-1.045
16	3.382E3	3.505E3	-3.622

7. Conclusions For the case of tapered bars, it has been demonstated that the modal synthesis approach, where substructures are assembled to form the overall structure, can be used at the element level itself. This approach has superior convergence characteristics and the advantages of hierarchical formulation.

8. References:

1. W. L. Heard Jr., H. G. Bush, R. E. Wallsom and J. K. Jensen. A mobile workstation concept for mechanically aided astronaut assembly of large trusses. *NASA Technical Paper 2108*, 1–35 (1983).

2. G. M. Lindberg. Vibration of nonuniform beams. *Aero. Quart.* **14**, 387 (1963).

3. K. E. Rouch and J. S. Kao. A tapered beam element for rotor dynamics analysis *J. Sou. Vib.* **66**, 119–140 (1979).

4. J. Thomas and E. Dokumaci. Improved finite elements for vibration analysis of tapered beams. *Aero. Quart.* **24**, 39–46 (1973).

5. T. W. S. To. Higher order tapered beam finite elements for vibration analysis. *J. Sou. Vib.* **63**, 33–50 (1979).

6. B. Ovunck. Dynamic analysis of frameworks by frequency dependent stiffness matrix approach. *Int. Assoc. Bridge Struct. Engg. Publ.* **32**, 137–154 (1972).

7. A. Avakian and D. E. Beskos. Use of dynamic stiffness influence coeffiecients in vibrations of nonuniform beams. *J. Sou. Vib.* **47**, 292–295 (1976).

8. A. K. Gupta. Frequency dependent matrices for tapered beams. *J. Struct. Div., ASCE* **112** 1–17 (1986).

9. J. R. Banerjee and F. W. Williams. Exact Bernoulli–Euler dynamic stiffness matrix for a range of tapered beams. Int. J. Num. Meth. Engg. **21**, 2289–2302 (1985).

10. C. C. Spyrakos and C. I. Chen. Power series expansions of dynamic stiffness matrices for tapered bars and shafts. *Inter. J. Num. Meth. Engg.* **30**, 259–270 (1990).

11. R. C. Engels. Reduced order structural modeling techniques for high energy laser systems. *Final report for AFWL/ARBM* Kirkland, NM (1986).

12. M. Link, J. Moreno–Barragan and M. Weiland. Derivation of finite element models using modal synthesis techniques. *Proc. Euro. Forum Aeroelas. Str. Dyn.. DGLR* Bonn (1989).

13. N. Ganesan and R. C. Engels. Hierarchical Bernoulli–Euler beam finite elements. *Comp. Struct.* (to appear) (1992).

14. N. Ganesan and R. C. Engels. Timoshenko beam finite elements using assumed modes method. *J. Sou. Vib.* (to appear) (1992).